Nature Water, Volume 2, June 2024, pp. 553-565
DOI:10.1038/s44221-024-00249-y

Viral metagenome reveals microbial hosts and the associated antibiotic resistome on microplastics

Ruilong Li[1,2†], Xin-Li An[1†], Yijin Wang[2], Zhugen Yang[4], Jian-Qiang Su[1], Jonathan Cooper[5], Yong-Guan Zhu[1,3*]

[1]Key Lab of Urban Environment and Health, Institute of Urban Environment, Chinese Academy of Sciences, Xiamen 361021, China

[2]College of Light Industry and Food Engineering, Guangxi University, Nanning 530004, China

[3]State Key Lab of Urban and Regional Ecology, Research Center for Eco-Environmental Sciences, Chinese Academy of Sciences, Beijing 100085, China

[4]School of Water, Energy and Environment, Cranfield University, Cranfield, MK43 0AL, United Kingdom

[5]The School of Engineering, The University of Glasgow, G12 8LT, United Kingdom

[†] These authors contributed equally to this work.

[*]Correspondence should be addressed to: ygzhu@rcees.ac.cn (Yong-Guan Zhu).

Abstract

Microplastics provide a unique niche for viruses, promoting viral interactions with hosts and accelerating the rapid "horizontal" spread of antibiotic resistance genes (ARGs). Currently, however, there is a lack of knowledge concerning the main drivers for viral distribution on microplastics and on the resulting patterns of viral biogeographic distributions, and the spread of the associated ARGs. Here, we performed metagenomic and virus enrichment-based viromic sequencings on both polyethylene (PE) and polypropylene (PP) microplastics along a river. Experimental results show that *Proteobacteria*, *Firmicutes*, *Actinobacteria* and *Cyanobacteria* were the potential hosts of viruses on microplastics, but only approximately 4.1% of viral variations were associated with bacterial community. Notably, two shared ARGs and six metal resistance genes were identified in both viral and their host bacterial genomes, indicating the occurrence of horizontal gene transfer (HGT) between viruses and bacteria. Furthermore, microplastics introduce more distinctive elements to viral ecology, fostering viral diversification and virus-host linkage while refraining from an escalated level of HGT of ARGs, in contrast to natural matrixes. Our study provide comprehensive profiles of viral communities, virus-related ARGs and their driving factors on microplastics, highlighting how these anthropogenic niches providing unique interfaces that comprise highly defined viral ecological features in the environment.

Keywords: Microplastics, Antibiotic resistance genes, Virus, Horizontal gene transfer, Host bacterial genomes

Introduction

Published by Springer. This is the Author Accepted Manuscript.
The final published version (version of record) is available online at DOI:10.1038/s44221-024-00249-y. Please refer to any applicable publisher terms of use.

Persistent and cyclic microplastics pollution has been considered as a hallmark of the anthropocene[1]. This increasing stream of human-made polymers are becoming an emerging environmental and human health crisis, posing toxic effects by releasing leachates and even threatening human health via directly entering biological tissues and cells or trophic transfer[2-4]. Research efforts have unraveled microplastics provide a novel niche for microbial colonization and biofilm growth, owing to their high hydrophobicity, large surface/volume ratios, persistence and recalcitrance[5, 6]. The diverse microbial community of heterotrophs, autotrophs, predators, and symbionts that colonize microplastics has become known as the "plastisphere"[7]. Evidences that microplastics surfaces selectively enrich pathogens into areas inaccessible to natural substrates suggest that MP pollution could provide new refuges for pathogens and have ramifications on disease transmission and treatment[8, 9].

Viruses are ubiquitous and abundant members of Earth's microbiomes, impacting host evolution, metabolism, and Earth's biogeochemical cycles. However, most studies of plastisphere have overlooked viruses while largely focusing on bacteria and fungi. A few studies on virions on microplastics have shown that viruses can hitchhike on microplastics and prolong their infectivity by adhering to the microplastics surface, which have not investigated viral communities and their bacterial hosts[10-12].Our recent study that applied bulk metagenomic sequencing provided evidence that viruses are ubiquitous on microplastics surfaces in a freshwater environment[13]. Antimicrobial resistance bacteria are a compelling health issue since they make antibiotic treatments obsolete, even causing the death. Although studies have characterized the resistome in the plastisphere[8, 13, 14] and analyzed the presence of antimicrobial resistance genes (ARGs) in the viral fractions from various environmental compartments, microplastics associated viruses-host interactions have not yet been reported[15, 16]. It has been argued

that the abundance of phage-borne ARGs has been overestimated due to the rare occurrence of phage-mediated ARG transduction and the contamination with nonviral DNA (free bacterial DNA or outer membrane vesicles)[15, 17]. However, recent advances in viral particle enrichment and bioinformatic tools for viromes have enabled the recovery of a vast richness of viral populations and accurate prediction of the association between viruses and their potential bacterial hosts in the plastisphere.

Microplastics have been posited to act as a new substrate within aquatic environments, with MP-associated bacterial communities found to be distinct from those in naturally occurring substrates[18]. The synthetic polymers show extensively higher microbial community richness and evenness than the surrounding natural substrates (i.e. water, sediment, wood, cobblestone, rock, and leaf) (Ogonowski et al., 2018; Wang et al., 2020; Zadjelovic et al., 2023). Evidences of niche partitioning between different polymer types have observed that microplastics harbour communities discrete from other polymer types (i.e. cellulose and glass beads)[19]. The physicochemical properties, surrounding nutrients, and pH can affect the abundance, diversity, and activity of biofilm microbial communities on these substrates[20-22]. Additionally, viruses as mobile genetic elements may alter the adaptive evolution of their hosts, and promote nutrient cycling and microbial diversity via killing their host[23, 24]. Bacterial populations may act as biotic factors that regulate the viral ecology via host-virus interations[25, 26]. Under the substantial pressure imposed by myriad abiotic and biotic variables, viromes and their associated ARGs on plastisphere are expected to exhibit significant divergence from the surrounding substrates. To test this hypothesis, our study extracted microbial DNA and viral DNA from the surfaces of microplastics (polyethylene and polypropylene), stone, wood and sand. Metagenomic sequencing and viral particle enrichment-based viromic sequencing were applied to explore the unique

viral community on microplastics, their associated ARGs, and the factors driving changes in the plastisphere. The data would provide a benchmark for assessing the potential of horizontal gene transfer and environmental risks of viral communities in the plastisphere.

Main text

Diversity of Bacterial Communities on Microplastics

A total of 28,732 bacterial species were obtained in microplastic samples at the watershed scale using metagenomic sequencing. *Proteobacteria*, *Acidobacteria*, *Actinobacteria*, and *Chlorobacteria* were the dominant phyla in both PP and PE, accounting for 52.60% of the total bacterial community (Fig. S2a). No significant difference in both the species richness (ACE, Chao1 and Richness index) and evenness (Shannon, Simpson and Pielou indexes) was found with sampling sites (from site1 to site 5) or microplastic types ($P > 0.05$, Fig. S2c and S6b). The core bacterial community was also evaluated across all samples. A set of 25,883 bacterial species were found in all sampling sites, and the core species accounted for 78.4 % of the total bacterial species detected. As shown in the Venn diagram, there were 12,284 bacterial species shared in all the samples expect the sample PE_5 with lowest species richness (Fig. S3). A majority of bacterial species (28599) were shared between microplastic types, and there were 49 and 84 species were only in PE and PP, respectively (Fig. S2d).

Approximately 0.32% of bacterial species were identified to be potential pathogens. A total of 91 species of potential pathogenic bacteria were detected, which belonged to 11 phyla (Fig. S13a). No significant difference was detected with sampling sites or plastic types (Fig. S13b and S13c). On these microplastics, *Burkholderia cepacia* (13.29%), *Klebsiella pneumoniae* (10.21%) and *Clostridium sp* (7.59%) were

126 the dominant detected pathogens.

127 A significant distance-decay effect was also observed in the similarity of microbial
128 community composition between any two sampling sites (R^2 = 0.842, P < 0.001) (Fig.
129 S2b). NMDS analysis showed that no geographical cluster of bacterial communities
130 was observed among the samples, and the distribution of bacterial community in the PE
131 samples was significantly different from the one in the PP microplastics (P < 0.05) (Fig.
132 S2e).

133

134 **Diversity of Viral Communities on Microplastics**

135 A total of 226,853 contig fragments were obtained, of which the contig length less
136 than 1000 kb accounted for 89% of total contigs (Fig. S4a and Table S2). 17,180, 38,029
137 and 17,4331 assembled contigs were assigned to viral genus, family and order level,
138 respectively (Fig. S4b-d). *Myoviridae* and *Siphoviridae* were the dominant viral
139 communities at the family level, accounting for 58.8% of the total viral abundance in
140 all samples (Fig. 1a). No significant difference in the richness and evenness of viral
141 community was found with microplastic types (P > 0.05, Fig. 1c and S6a). Assembled
142 viral contigs were classified into 501 viral genera, and 364 viral genera shared among
143 these two kinds of microplastics (Fig. 1d), in which *Asteriusvirus* (25.46%),
144 *Prasinovirus* (4.60%), *Klosneuvirus* (4.22%), *Peduovirus* (3.86%), *Mimivirus* (3.70%),
145 *Punavirus* (3.34%), *Chlorovirus* (3.11%) and *Salacisavirus* (3.03%) were the dominant
146 genera (Fig. S8).

147 A significant distance-decay effect was also observed in the viral communities
148 between any two sampling sites (Fig. 1b). NMDS analysis based on Bray-Curtis
149 distance revealed the distinct dissimilarity of viral communities between PE and PP
150 microplastics (P < 0.05) (Fig. 1e).

151

152 **Bacterial and Viral Resistance Genes on Microplastics**

153 The functional genes of both bacterial and viral sequences were annotated on the
154 microplastics at the watershed scale, based on blasting against the UniProtKB, KEGG,
155 BacMet and SARG databases (Fig. S9a and S9d). Most of the viral genes
156 (approximately 58.75% of predicted ORFs) were annotated as "unclassified and poorly
157 characterized" using KEGG database, while other genes (15.38% of ORFs) were
158 mainly belonging to protein families of genetic information processing, protein families
159 of signaling and cellular processes and nucleotide metabolism and unclassified genetic
160 information processing at KEGG level 2. Moreover, 11.91% of predicted viral ORFs
161 were successfully annotated against the UniPortKB database. The genes encoding
162 technical terms, molecular function and biological process accounted for 10.33%, 8.48%
163 and 7.51% of the total viral ORFs, respectively.

164 For bacterial functional genes, a majority of unigenes (59.52%) were unclassified
165 and poorly characterized, and some other unigenes were associated with metabolic
166 pathways (11.88%), biosynthesis of secondary metabolites (5.43%), microbial
167 metabolism in diverse environments (3.72%) and biosynthesis of amino acids (2.18%).
168 No distinct distribution patterns of bacterial or viral functional genes were observed
169 with the microplastic types ($P > 0.05$) (Fig. S9b), whilst the similarity of the distribution
170 of the bacterial functional genes was significantly decreased with the increasing
171 geographical distance ($P < 0.05$) (Fig. S9c and S9f).

172 A total of 779 viral ORFs were found to carry 72 metal resistance genes (MRGs),
173 of which 31 metal resistance types were shared in all samples. 21 metal resistance types
174 were shared in both microplastic types and 14 metal resistance types were shared in 5
175 sampling sites. The five most dominant shared metal resistance types conferred

resistance to Cu (15.11%), Zn (13.98%), As (10.70%), Fe (9.98%), W and Mo (6.77%) (Fig. 2a). For bacterial community, sixty-eight metal resistance types consisting of 391 MRGs (41393 bacterial unigenes) were detected in bacterial metagenomes. MRGs in bacterial metagenomes mainly encoded resistance to Cu (15.11%), Zn (13.98%), As (10.70%) and Fe (9.98%) (Fig. 2b). Sixty-five metal resistance types were shared in both plastic types whilst 57 MRG resistance types were shared among the sampling sites. It is notable that bacterial metagenomes exhibited 39 unique metal resistance types, whereas no unique metal resistance type was detected in virome.

Fifty-seven ARG subtypes (667 viral contigs) conferring resistance to 13 antibiotic classes were detected based on virome data, and there were 34 ARG subtypes shared in both PE and PP microplastics and 19 ARG subtypes shared in 5 sampling sites. Among these ARGs, trimethoprim (33.19%), tetracycline (21.55%), and MLS (19.62%) resistant genes were the most abundant ARGs. All common resistance mechanisms were detected, including antibiotic efflux (39.98%), antibiotic target replacement (33.19%) and antibiotic target protection (17.88%). Regarding bacterial metagenome, 210 ARG subtypes (11,443 bacterial unigenes) were detected to encode resistance to 20 antibiotic types. Among these bacterial ARG subtypes, 166 ARGs (encoding resistance to 19 drug classes) were shared in both PE and PP microplastics and 104 ARGs (coding resistance to 17 drug types) were shared in 5 sampling sites. ARGs encoding resistance to multidrug (33.73%), macrolide-lincosamide-streptogramin (MLS) (23.82%), and tetracycline (13.64%) were the most abundant. All common resistance mechanisms were observed and antibiotic efflux (77.27%)-related ARGs accounted for the highest proportion of the detected ARGs. No significant variation for viral ARGs and MRGs composition was observed along geographical distance gradient (ANOVA, $P > 0.05$), while bacterial ARGs and MRGs distribution exhibited distinct differences with the

increasing distances (Fig. S9). In the metagenome, a total of 22,992 unigenes were associated with MGEs, including transposon (73.55%), recombinase (19.80 %), and integron (6.65%). There was no significant difference in MGE abundance between different sampling sites and microplastic types (ANOVA, $P > 0.05$).

Drivers of Viral Community and Resistance Genes Distribution

The abundance (Pearson's, right triangle) and compositions (Mantel test, left link) of virus species, ARGs, and MRGs were not significantly correlated with almost all non-biological environmental and biological factors (bacterial community species and functional genes) ($P > 0.05$) (Fig. 3a). A majority of variations in viral ARG (92.2%) and MRG (98.0%) compositions were unable to be explained by abiotic factors (metal concentration, antibiotic concentration, geographical distance, salinity, and etc.) and biotic factors (bacterial community and MGEs), Fig. 3b and 3c. Only 7.7% of variation in viral taxonomic composition was explained by physicochemical properties (3.2%) and bacterial community (4.1%), while approximately 92.3% of viral variation can be unexplainable (Fig. 3d).

For the bacterial community, the abundance and composition of bacterial species, ARGs and MRGs were significantly correlated with most environmental factors (e.g. metal concentration, antibiotic concentration, geographical distance, salinity, dissolved oxygen, chemical oxygen demand, biological oxygen demand, flow rate, ammonium nitrogen, total phosphorus, total nitrogen, dissolved organic carbon, pH, and urbanization factors, $P < 0.05$, Fig. 3a). Abiotic factors and viral community (19.3%) commonly explained 21.1% of variations in bacterial community, while 78.9% of variations were not explained (Fig. 3e). MGEs could explain 60.6% of the variations of bacterial ARG composition and 8.8% of the variations of bacterial MRG composition,

226 respectively, Fig. 3f and 3g.

227

228 **Interaction between Viral Community and Host Bacteria**

229 *Viral and Bacterial Species*

230 Based upon the approaches of tRNA matches, clustered regularly interspaced short
231 palindromic repeats (CRISPR) spacer linkages and direct nucleotide alignment by using
232 blastn, a total of 1,491 host-virus pairs were linked in the samples, and the number of
233 associations in PP (1,001 pairs) were almost two times as much as the one in PE (490
234 pairs) (Supplementary Data 2). Only 4.94% viral contigs (mostly assigned to 28 viral
235 families) of the total contigs were associated with these predicted host-virus pairs, and
236 594 viral associated scaffolds could only be annotated at the kingdom level (Fig. 4a).
237 Most of the predicted host populations associated with the host-virus pairs were
238 assigned to five phyla, including *Proteobacteria* (761), *Actinobacteria* (79), *Firmicutes*
239 (34), *Cyanobacteria* (17), and *Bacteroidetes* (6), Fig. 4a.

240 Pearson analysis showed that two shared and diverse host bacterial phyla
241 (Proteobacteria and Actinobacteria) showed significant correlations with the
242 abundances of viral contigs, $P < 0.01$, Fig. 4b. Furthermore, the virus-host abundance
243 ratios were calculated to assess how virus-host dynamics varied across different hosts
244 and virus-host abundance ratios (typically > 1) were observed among different hosts,
245 and the highest average values were observed in Proteobacteria and Actinobacteria (Fig.
246 4b). The abundances of the host phyla were significantly correlated with the total
247 abundance of viruses infecting the same host lineage on microplastics ($R^2 = 0.991$, $P <$
248 0.001), Fig. 4c.

249 *Shared resistance genes*

250 Virus-host pairs prediction analysis showed that six MRGs including *pfr* (Fe, Cu,

Mn), *copF* (Cu), *arsB* (As), *zraR*/*hydH* (Zn), *pitA* (Zn, Te) and *modC* (W, Mo) and two ARGs (*bla*$_{OXA}$-9 encoding β-lactamase) and *dfrA*1 encoding resistance to trimethoprim) were detected in both the viruses and their host bacteria. Relative abundances of shared ARGs and MRGs in the virus-host pairs were calculated by mapping viral clean reads to the resistance gene-associated contigs. These shared resistance genes (MRGs and ARGs) were mainly carried by the class *Caudovirales*, *Imitervirales* and unclassified viral class (Fig. 4d). The potential bacterial hosts of the shared MRGs were frequently associated with *Pseudomonadaceae*, *Flavobacteriaceae*, *Mycobacteriaceae* and *Comamonadaceae*. The two shared ARGs *blaOXA*-9 and *dfrA*1 had the bacterial hosts related to *Comamonadaceae*.

Comparisons plastisphere and natural particles

Taxonomic composition

By employing metagenomic sequencings on 11 natural particles (3 for stone, 4 for wood, and 4 for sand) from corresponding sampling sites, 10761 viral contigs were obtained, respectively. After taxonomically identified by referencing IMG/VR database by using VPF-Class, 6177 of these vOTUs were assigned to family level, respectively.

Viral community taxonomic composition has significant divergence between samples from distinct compartments (Fig. 5). Myoviridae, Siphoviridae, and Mimiviridae dominated the plastisphere viral communities at family level in microplastics, whereas the viral communities in natural particles were dominated by *Myoviridae*, *Siphoviridae*, and *Podoviridae*. Additionally, regarding viral community alpha diversity (Fig. 5c, d, f, and g), samples collected from natural particles showed much higher viral richness and evenness compared to microplastics from the Beilun River, where the wood has the highest viral richness and evenness.

Resistance genomes and host prediction

Viral open reading frames (ORFs) were assigned to functional genes by referencing eggNOG database. Compared with the uniform viral functional profiles in natural particles, there were less abundant and less diverse viral functional genes in plastisphere, especially for PE (Fig. 5 b and Fig. S14). Either functional gene or ARG profiles exhibited a significant clustering pattern according to the type of material types among distinct samples (Fig. 5 e and h).

To assess the viruses-associated microbiological risks, we identified the viral ARGs by referencing SARG database. As a result, we respectively identified 9356 MRGs (conferring resistance to 58 types of metals) and 455 MRGs (conferring resistance to 25 types of metals) (Fig. S15 and Fig. S16). It was found that microplastics had much lower abundance and diversity of MRGs , but wood posed the highest viral metal resistance associated risks, followed by sand, stone, PE, and PP. Moreover, 525 ARG subtypes (12831 ARGs) and 163 ARG subtypes (3379 ARGs) were found from both natural particles and microplastics samples, which dominantly conferred resistance to 26 types of antibiotics (Fig. S17 and Fig. S16). Notably, significant higher abundances of ARGs were found in sand, whereas the ARG abundances of other samples followed the order: Wood > PP > PE > Stone (Fig. S17a). The type of particles may also determine the prevalent ARG types (Fig. S17a). That is, rifamycin, MLS, multidrug, and tetracycline were the dominant ARG types from natural particles, where aminocoumain and tetracycline dominated the ARG types of microplastics. This phenomenon is associated with the distribution of resistance mechanism, where efflux pump, antibiotic target protection, and regulator dominated natural particles resistance mechanism. However, themutation, antibiotic target protection, and antibiotic target

alteration relies on the resistance mechanism of the microplastics samples (Fig. S17b).

By comparing the nucleotide similarity of CRISPR-spacers and tRNA in both viromes and metagenomic assembled genomes (MAGs), we predicted the potential linkage between the viral contigs and their hosts' MAGs. Consequently, the hosts of 1589, 870, 515, 285, and 612 viral contigs were successfully predicted for stone, wood, sand, PE and PP, respectively (Fig. S19). Significantly diverse virus-host pairs were found in natural particles rather than plastisphere.

Furthermore, we delineated the occurrence of horizontal gene transfer (HGT) between viruses and their hosts by identifying the coexistence of specific ARGs in both viral contigs and their predicted host scaffolds, which were observed in both microplastics and sediments. HGTs of MRGs occurred more prevalently in samples from Beilun River, with 5 MRGs found in PE and 1 MRG in PP, than in sand samples (only 1 MRG found in wood). Neither MRG performed HGT in other natural samples nor horizontally transferred MRG were shared among samples (Fig. S20a). HGTs of ARGs occurred more prevalently in sediments (6 ARGs in sand) than in microplastics (6 ARGs in stone, 2 ARGs in wood, 2 ARGs in PP, and no ARG in PE). It is worth noting that the HGT of an ARG (i.e. rsmA conferring resistance to diaminopyrimidine) was observed in three kinds of natural particles, whereas no shared HGTs of specific ARG was obtained between microplastics and other natural particles (Fig. S20b).

Virus in microplastics collected from river watershed

Microplastics provide a distinct human-made niche for colonization, proliferation and genetic exchange of viruses and their bacterial hosts. These microbial hitchhiker niches, such as pathogens or ARGs, hosted by microplastics, can spread to other environments either by water flow or water columns in the river. In this study, the

326 microplastics were collected from the Bei-Lun River watershed throughout the
327 geographically Karstic areas. Our data showed that microplastics in the river can host
328 a diversity of bacterial and viral communities using the combination of metagenome
329 and virus-enriched virome sequencing. Recent studies have demonstrated that the viral
330 contings deriving from metagenome sequencing alone are far less than those from the
331 viromes, which is not sufficient to reveal the viral taxonomic and functional diversity
332 in the complex environments, especially for the rare taxa[13, 27]. Compared to merely
333 42174 viral reads and 11 ARGs in viromes priorly identified from total plastisphere
334 metagenomes without viral purification, the combined approach used in this study can
335 override the metagenome sequencing since metagenome sequencing depth from
336 microplastics might limit the interpretation of the viral biodiversity[13]. Moreover, viral
337 enrichment is challenging the possibility of identifying the viral contigs. Our present
338 study showed that viral enrichment-based virome sequencing was able to capture more
339 viral species and functional genes. Therefore, the combination of metagenome and
340 virome sequencing data can provide a comprehensive profile of the diversity of viral
341 communities, host-viral associations and the potential HGT of ARGs on microplastics.
342 No significant difference in the Alpha diversity of microbial or viral communities
343 was observed in the different sampling sites and different types of microplastics. This
344 was possibly attributed to biofilms on microplastics, providing a stable shelter for
345 microbial and viral colonization. Both microbial and viral communities showed no
346 distinct cluster with sampling sites, while the community structure of PE and PP was
347 significantly different. The selective adsorption of microorganisms onto microplastics
348 possibly explained the distribution heterogeneity of microbial and viral communities
349 on microplastics with different materials. PE has a larger specific surface area than PP,
350 which is favorable for bacterial adhesion. The alanine, aspartate and glutamate

metabolism-related genes are enriched in the viral metagenome of PP, further indicating that PP microplastics might be feasible to microbial and viral proliferation and metabolism on PP. The biogeographic pattern that community similarity decreases with increasing geographical distance has been observed in both microbial and viral communities. One possible reason was that the interaction between viruses and their bacterial hosts might contribute to the elimination and replacement of species in reassembling processes of microbial populations.

Microbial community composition showed that *Proteobacteria*, *Acidobacteria*, *Actinobacteria*, and *Chlorobacteria* were found to be the dominant bacterial phyla on PP and PE microplastics from the Bei-Lun River. The observation was consistent with previous studies in rivers, lakes, soils, oceans, wastewater treatment plants, polar regions, and deep-sea environments[28, 29]. Some potential pathogens including *Burkholderia cepacia*, *Klebsiella pneumoniae* and *Pseudomonas aeruginosa* were also detected on microplastics, indicating that these pathogens could infect humans and animals by hitching a ride on microplastics to other environments. For viral community, *Myoviridae* and *Siphoviridae* were found to be predominant viral families on microplastics, which were also reported to be abundant in agricultural soils, marine and river[30-32]. Additionally, MDA is known to introduce biases associated with sequence composition[33], which might partially explain the high abundance of the typical dsDNA viruse *Myoviridae* on the microplastics.

Previous studies have demonstrated that the microplastics act as hotspots of ARGs[8, 34]. Our findings provides new knowledge and understanding of ARGs and MRGs of plastisphere based on the metagenome and virome data and its role in the spread of AMR through HGT. Our study found that only 667 viral contigs carried ARGs, accounting a small proportion of total contigs, which was consistent with the previous

studies. Trimethoprim, tetracycline, MLS resistance genes were frequently detected in the viral contigs. Previous studies observed the trimethoprim, chloramphenicol and MLS resistance genes frequently in soils, the polymyxin resistance proteins mostly in rivers, and beta-lactamase in swine gut[16, 35]. One possible explanation was that the ARG distribution associated with the viruses linked to their surrounding environments.

Bacterial ARGs on microplastics were observed to mainly encode resistance to multidrug, MLS, and tetracycline, which was different from our previous high through qPCR research. The data mainly were attributed to the difference in the used approach for detecting ARGs on microplastics. In this study, some MRGs were also detected in viral and bacterial sequences on plastisphere. Al and Fe resistance genes accounted for a large proportion of MRGs of virome, while bacterial MRGs were mainly associated with the resistance to Cu, Zn and As[36, 37]. These auxiliary metabolic genes might be favorable for the hosts' adaptation to stressed environments via compensating for host bacterial metabolism outputs.

Abiotic factors and viral community contributed to the distribution of bacterial community on microplastics, indicating the potential Interactions between bacterial and phage communities in natural environments. The large proportion of unexplained variance needs to be further investigated in the future study. MGEs including transposon, recombinase and integron were frequently detected in the bacterial contigs, and MGEs and this was partially associated with bacterial ARGs and MRGs distributions. This was expectable that horizontal transfer of ARGs and MRGs was frequently mediated by MGEs. Bacterial community exerted marginal effect on viral community. Environmental factors, including pH, salinity and nutrient concentration, have been confirmed as the dominant factors governing the viral community and their carried resistance genes on microplastics, which was consistent with the finding in

marine sediment, agricultural soils and even mine drainage sediments[28, 29]. Previous metagenomics data have also demonstrated that anthropogenic activity indicators, geographic distance and microplastics types are the major drivers of bacterial abundance and diversity of resistance genes in water and soil/sediment[34, 38, 39]. However, this study found that no significant association was observed between virial ARG, MRG, taxonomic composition and individual environmental factors. One possible explanation was that the limited exchange of organic and inorganic matter between water and polymer might exerted little impact on the structure and compositions of viral community of plastisphere. Furthermore, non-polar microenvironment of microplastics might reduce the colonization of bacteria, and thus exacerbated their dependences of phages.

Proteobacteria, *Actinobacteria*, *Firmicutes*, and *Cyanobacteria* were the domain potential host phyla of microplastic viruses based on metagenomic binning data. The abundance of almost all viruses exhibited similar variations to that of their hosts. Previous studies also observed that *Proteobacteria*, *Actinobacteria*, *Firmicutes*, and *Cyanobacteria* were the domain potential host phyla of plastisphere, ocean, soil viruses. *Terapinvirus*, *Omegavirus*, *Cafeteria* and *Prasinovirus* were the most frequently detected with the potential hosts. *Terapinvirus*, a genus of dsDNA virus in the class Caudoviricetes, has been reported to be bacterial and archaeal viruses[39]. *Omegavirus* were potential wide-host viruses, which were identified with the potential hosts from Proteobacteria and Firmicutes. A previous study has found that *Mycobacteria,* human pathogens, are their natural hosts. *Cafeteria* was a giant virus with a remarkable complement of genes infects marine zooplankton[45], and that both Proteobacteria, Actinobacteria were its potential hosts. It has also been shown that *Prasinovirus* can infect the algae in the freshwater environment, and our study further demonstrates that

freshwater is its preferring niche[27].

Comparisons of plastisphere and natural particles

Some interesting phenomena were observed in the comparisons of microplastics and other natural particles, which would shed light on the dynamics of host microbial-viral migration. Various viruses were identified in each plastisphere derived from the Beilun River, but their richness and diversity were significantly lower than those identified in natural particles. This has been supported by the following evidence. Firstly, previously reported as numerous as bacteria in various biotopes[40, 41], viruses and the assemblages they compose more diversified in natural particles, which could be influenced by the distinct nutrient availability in different habitats. Further in support of this, capable of governing viral hosts' life strategies, viral auxiliary metabolic genes (AMGs) exhibited significantly higher abundances in natural particles compartments compared to plastispheres. Secondly, unlike bulk soils with ample resources, plastispheres always have uncontrollable and harsh environmental conditions comprising the variable interior volumes and shapes of microplastics, the persistent and substantial properties of microplastics against decomposition, as well as a vast range of toxic leachates[42]. These unfavorable conditions, together with the properties of surface materials, can drive taxonomic variations and functional shifts in the viral and their hosts' microbiomes[43]. It is worth noting that, in order to be adapted to the harsher conditions, viruses in microplastics are prone to have a broader host range, which have been supported by ecological evidence that environmental filtering can limit the diversity of viruses but improve their hosts' range[44].

Additionally, in contrast to the previous reports considering that plastispheres often exhibit higher HGTs of ARGs than natural matrixes merely according to the

abundant and diverse MGEs found in plastispheres[45, 46], sediments exhibited more prevalent virus-mediated HGTs of ARGs than plastispheres in this study directly supported by genetic evidence. This phenomenon could be ascribed to the generally higher accumulation of antibiotics in natural water and sediments than in microplastics, fitting quite well to the hypothesis "cost of antibiotic resistance"[47, 48]. microplastics is hence capable of providing a favorable niche for viral diversification and virus-mediated HGT of ARGs. As we know plastisphere bacteria typically significantly response to environmental variables, instand the relatively enclosed circumstance of plastisphere enables the robustness and uniqueness of viral communities, viral ARGs, and virus-host linkages, as the more highly linked virus-host relationship unraveled in microplastics compared to natural particles.

The results improve our understanding of the potential host of viruses and the virus-host relationships in microplastics, although a majority of bacterial hosts could not be identified at the low taxonomic levels (e.g., at the genus level). The shared resistance genes were observed in both bacterial and viral contigs, indicating that viral particles might exert a potential role in the HGT of resistance genomes. The data may be attributed to the microplastics biofilm providing favorable micro-environment for the genetic exchange between bacterial and viral genome due to infection.

Our findings also provide a comprehensive profile of the viral community patterns, ARGs and MRGs, virus-host interactions and driving factors based metagenomic and viromic sequencing. More importantly, some unique features of viral diversity and shared resistance genomes with their host bacteria through HGT were detected in microplastics along the river, in comparisons to natural particles (sand, wood and stone). Four resistance genes are shared by virus and their hosts on microplastics, and the abundances are closely related to their geographical location. Moreover, dynamics of

viral populations and function are subjected to their hosts and have no close relationships with other environmental and anthropogenic factors, which is significantly different from other matrixes.

Methods

Sample Collection

Incubations of 30 days in situ of two types of microplastics, namely PE and PP were performed on March 2021 in the Beilun River (21° 32′- 22° 45′N, 107° 32′- 108° 03′E), Guangxi Province, China (Fig. S1 and Table S1)[22]. As an exorheic river of the Guangxi typical karst area, five sites along Beilun River were established for recovery of the immersed microplastics according to urbanization and physicochemical properties with Site 1 as the rural region, Site 2 and Site 3 as the peri-urban regions and Site 4 and Site 5 as being characteristic of urban regions.

On each site, 2.0g microplastic (PE and PP) and natural particles (stone, wood and sand) were cultured in river water, respectively. Detailed information is listed as follows. The characteristics of PE and PP microplastics were white fragment, where the size of PE was 0.90 ± 0.10 mm, and the size PP was 1.11 ± 0.15 mm, which were purchased from Aladdin Chemical Company (Shanghai, China). The microplastics were disinfected using 70% ethanol for 30 min and then rinsed exhaustively with sterile water. All of the natural particles are collected from the same zones in the upstream of Bei-Lun River, and immediately sterilized using high pressure steam sterilization pot to overcome the implication of the original bacterial and viral communities. And, only the extracted DNA concentration far less than 0.1 ng/μL and no band showed on the agarose gel can be considered as the qualified samples.

The incubation time was established based upon a previous study reporting the

501 successful biofilm formation on plastics within 30 days[49]. Particles were subsequently
502 placed at each site and persistently immersed in the water using techniques described
503 in our previous study[50]. After the incubation, microplastics, natural particles and 10 L
504 of water samples were collected at each site. All these samples were stored in sterile
505 glass containers and kept on ice at 4°C for transport, and finally stored at -20°C before
506 embarking the experiments.
507
508 **Measurement of Physicochemical Properties**
509 Large particles and potential herbivores were filtered using 10.0 and 3.0 μm filters
510 (Merck Millipore Ltd., Ireland), respectively. An inductively coupled plasma optical-
511 emission spectrometry (ICP-OES, Leeman, Prodigy) was used to determine the
512 concentrations of metals (i.e., Fe, As, Al, Te, Cu, Zn, Cr, Mn, Ni, Mo, V, W, Cs, Sn, Pb,
513 Ag, Co, Mg, Hg, Cd, Se, Ga, Na, K, Ca, Ba). A number of additional physicochemical
514 properties were collected, described in our previous studies, including particle size,
515 elemental composition, specific surface area, hydrophobicity, and zeta potential of
516 microplastics and the pH, DOC, TN, TP, NH_3-N, flow rates, BOD, COD and DO of the
517 local environment. The concentrations of diaminopyrimidines, tetracycline,
518 sulfonamides, fluoroquinolones, macrolides of the river water samples, and the levels
519 of urbanization (medical level, population size and domestic sewage discharge) were
520 also determined [13].
521
522 **Metagenomic Sequencing and Data Analysis**
523 DNA was extracted from microplastic and natural particles using a FastDNA Spin
524 kit (MP Bio) according to the manufacturer's instructions. The extracted DNA samples
525 were sent to Guangdong MAGIGENE Co., Ltd. (Guangzhou, China) for high-

throughput sequencing. Nine libraries with 400 bps insert size were constructed, and paired-end (PE, 2 × 150bp) sequencing was then performed on the HiSeq X platform (Illumina, San Diego, CA, USA). Approximately 550 million clean reads were obtained after quality screening by Cutadapt (v1.2.1)[51] and assembled by k-mer~ parameter settings (k-mer = 27, 127) of Megahit (v1.2.6) (https://hku-bal.github.io/megabox/)[52]. Prediction of open reading frames (ORFs) was performed using MetaGeneAnnotator[53], and then removal of redundant genes was performed using CD-HIT (v 4.8.1)[54] based on 90% sequence similarity and 90% coverage. High-quality reads were aligned to the non-redundant gene catalogs to calculate gene abundance with 95% identity using SOAPaligner (http://soap.genomics.org.cn/ version 2.21)[55]. Bacterial reads were initially retrieved from by using Kraken2, and subsequent to this, assembled into bacterial genomes. The metagenomic binning was conducted by using MetaWrap2, with parameters set at 50% completeness and 10% contamination. This comprehensive approach aimed to efficiently recover bacterial genomic information, ensuring a robust analysis of the dataset. Bacterial taxonomic annotation was performed by BLASTn against NCBI-NT database (Nucleotide collection, ftp://ftp.ncbi.nih.gov/blast/db/, v2016-6-19, E-value ≤ 10^{-5}) using the lowest common ancestor (LCA) algorithm in MEGAN 5[56].

Viral DNA Extraction and Sequencing

The detachment of microbes from microplastics and natural particles was performed using methods according to Yang et al.[49] by vigorous vortex for 5 min in 5 mL PBS supplemented with 0.5% (v/v) Tween 20 (Aladdin). Microbial biomass was collected and microplastics were then eluted with sterile water. After centrifugation and washing with sterile water, the extraction of viral DNA was performed according to the

551 method described by Trubl et al.[57] and Adriaenssens et al.[58] with the following
552 modifications. In brief, the buffer containing microbes detached from microplastics
553 were homogenized and then filtered through a 0.25 mm filter membrane
554 (Biosharp,USA). The filtrate was mixed with 1% potassium citrate buffer by weight
555 (10 g L^{-1} $C_6H_5K_3O_7$, 1.92 g L^{-1} $Na_2HPO_4 \cdot 12H_2O$ and 0.24 g L^{-1} KH_2PO_4; pH = 7)
556 (Sigma-Aldrich, USA). The mixture was first incubated at 4°C for 15 min, and then
557 sonicated (100 W, 47 kHz) on ice for 3 min with manual shaking for 30 secs per minute.
558 After the first centrifugation (4602 xg for 10 min) (eppendorf, Centrifuge 5420), the
559 supernatant was transferred to a second tube and re-centrifuged again at 5478 xg for 15
560 min. The resultant supernatants were sequentially filtered through 0.45 and 0.22 μm
561 filters (Anpel Hydrophilic PTFE Syringe Filters, China) to remove the remaining non-
562 viral-like particles.

563 Extracts were enriched using tangential flow filtration technique (TFF, Sartorius
564 Vivaflow50 30,000 MWCO PES, USA). The concentrated samples were precipitated
565 with PEG-8000 (10% w/v) (Solarbio, P8260) and incubated overnight at 4 ℃. Viral
566 particles in precipitation were centrifuged by cesium chloride density gradient (1.7, 1.5,
567 and 1.35 g/mL layers) and particles in 1.35-1.5 g mL^{-1} layers were collected.
568 Subsequently, the purity and morphology of virus samples were examined by 1% uranyl
569 acetate staining (FEI Tecnai G2 Spirit Bio TWIN, USA) under a transmission electron
570 microscopy (TEM). Enriched viral particles were treated with DNase I [TaKaRa
571 Recombinant DNase I (RNase-free) 2270A] and RNase A (Takara Ribonuclease A 2158)
572 to remove non-encapsulated DNA and RNA fragments, respectively. The presence of
573 bacterial DNA was evaluated by PCR of 16S rRNA gene. The solution was then
574 subjected to viral DNA extraction using a Takara MiniBEST Viral RNA/DNA
575 Extraction Kit Ver.5.0 and the concentration of viral DNA was determined using a Qubit

576 3.0 fluorometer (Invitrogen, Waltham, Massachusetts).

577 Multiple displacement amplification (MDA) was performed for the extracted viral
578 DNA to meet metagenomic sequencing requirements. It should be noted that this
579 approach may introduce unavoidable but small sequencing biases. Nine amplification
580 products were sent for metagenomic sequencing using the HiSeq 4000 platform
581 (Illumina, San Diego, CA, USA) and each 400bp insert size fragment library yielded
582 150bp paired end reads.

583

584 **Virus Identification**

585 After quality control with Trimmomatic[59], a total of ~550 million clean reads (~55
586 million per sample) were used for the assembly of viral sequences to resolve potential
587 virus clusters on microplastics using Megahit (v1.1.2) with parameters of -presets meta-
588 large-min-contig-len 300. Totally, 4,997,260 and 5,578,389 contigs were recovered
589 from PE and PP samples, respectively. Potential viral contigs were initially predicted
590 through the "Prodigal" package in CheckV[56], and were further processed by the virus
591 hidden Markov models (vHMMs) pipeline to identify microbial and viral genes using
592 three different filtering criteria, namely: (i) the score of gene identification must be
593 greater than 1.2; (ii) if the sequence contained 10 genes, the host sequence was
594 determined to contain at least 2 microbial genes while the viral sequence was
595 determined to contain at least 2 viral genes, and; (iii) as host sequences, at least 30% of
596 the genes should be annotated as microbial genes. The potential viral contigs with high
597 confidence identified by VirSorter2 (v 1.0.5) were involved. Consequently, 226,853
598 unique contigs were assigned to viruses and 648 contigs were assigned to proviruses.
599 The host sequences in proviral contigs were cut out before taxonomic annotation.

600 Taxonomic annotations of viral contigs were assigned to putative virus dominant

(224986 contigs), phylum (174333 contigs), class (174331 contigs), order (174331 contigs), family (38029 contigs), genus (17810 contigs) and unassigned (1867 contigs) using VPF-Class[57] combined with CheckV. Clean reads were mapping to the resultant contigs using BWA (v0.7.17, mem -k 30) and the reads with the coverage < 80% were filtered. RPKM value (reads per kilo base per million mapped reads) for each contig was calculated to evaluate the viral abundance.

Host Prediction

The Quant_bin module of MetaWRAP (v1.3.2) was used to estimate the abundance of the constructed bacterial genome with default parameters[60]. Briefly, a per-sample assembly read (with clean reads) was generated using Salmon (v0.13.1)[61], which provides a table of relative abundance (genome copies per million reads (ppm)) for each scaffold in different samples. The abundance of contained bacterial alleles was summed and normalized to the total mapped reads across samples (genome copies/ppm reads) for each genomic bin. In this study, three computational strategies based upon nucleotide sequence similarity were used for host prediction, [62] namely:

(i) CRISPR spacer bar matching. CRISPR spacer sequences from the bacterial genome were predicted using a CRISPR recognition tool[63]. Detected spacer sequences were queried against the viral genome using the BLASTn-short function with the parameter of at least 95% identity over the entire spacer length, allowing only 1-2 SNPs at the 50 end of the sequence;

(ii) tRNA matching[57]. The "-t" option of ARAGORN[64] was applied to recover tRNAs from bacterial genomes and viral genomes, respectively. The recovered tRNAs were compared by BLASTn[65] and only exact

matches (100% length and 100% sequence identity) were considered as putative bacteria-virus pairs;

(iii) Nucleotide sequence homology between the bacterial genome and viral genome. The viral genome was queried against the bacterial genome using BLASTn[65]. Only alignments ⩾1000 bp in length with more than 70% coverage of the best hits indicated a bacteria-virus pair.

Functional gene annotation

Protein-coding sequences were predicted using PROKKA[66] and annotated by BLASTp against the Kyoto Encyclopedia of Genes and Genomes (KEGG) database, the unsupervised orthology group (eggNOG v5.0.0), the SARG database (http://smile.hku.hk/SARGs/), the BacMet database (http://bacmet.biomedicine.gu.se/) and the MGE database (https://bench.cs.vt.edu/ftp/data/databases/), with parameters of alignment = 1, threshold = 1e-10, and identity > 40%. Additionally, viral ORFs were annotated by BLASTp against the UniProtKB/Swiss-Prot (ViralZone, reviewed protein, https://viralzone.expasy.org/) with parameters of threshold = 1e-3. The annotation with the lowest E value in each database was then selected as the best hit for that protein. Pathogenic bacteria were screened against a pathogen catalogue (Supplementary Data 1).

Statistical analysis

Statistical analysis and visualization of the data in this study was performed using R (v 4.1.1) (https://www.r-project.org/). Alpha and beta diversity analyses were performed using the vegan and ggplot2 packages in R. The degree of explanation (*R*-value) and significance (*p*-value) between samples were calculated based on Adonis

651 analysis (PERMANOVA). Adonis $R^2 = 0.99$ indicates that 99% of the between-sample
652 variation is explained, and a $p < 0.05$ value indicates high statistical significance. Stress
653 values < 0.05 for NMDS based upon Bray-Curtis distances indicate good agreement
654 between NMDS analyses, suggesting the consistence between the distances between
655 samples in a reduced two-dimensional space and the actual multivariate distances
656 between samples. LEfSe analysis was performed using the online Galaxy platform
657 (https://huttenhower.sph. harvard.edu/galaxy/). The definition of shared taxa or genes
658 was classified as three conditions, i.e., shared in all samples; shared in PP and PE
659 microplastics; shared in all five sampling sites, combing findings from both PP and PE
660 at the same sampling site.
661

662 **Data availability**

663 The raw sequencing reads of bacterial and viral communities have been deposited into
664 the NCBI Sequence Read Archive (SRA) under the accession number PRJNA1104113
665 and PRJNA1104403 (https://www.ncbi.nlm.nih.gov/sra). The other data generated in
666 this study are provided in the main text or Supplementary Information.
667

668 **Acknowledgements**

669 Yong-Guan Zhu's lab members were supported financially by the National Natural
670 Science Foundation of China (42021005, 22193061, 21922608), Key Collaborative
671 Research Program of the Alliance of International Science Organizations (ANSO-CR-
672 KP-2020-03, ANSO-PA-2020-18), and Chinese Academy of Sciences (ZDBS-LY-
673 DQC027).

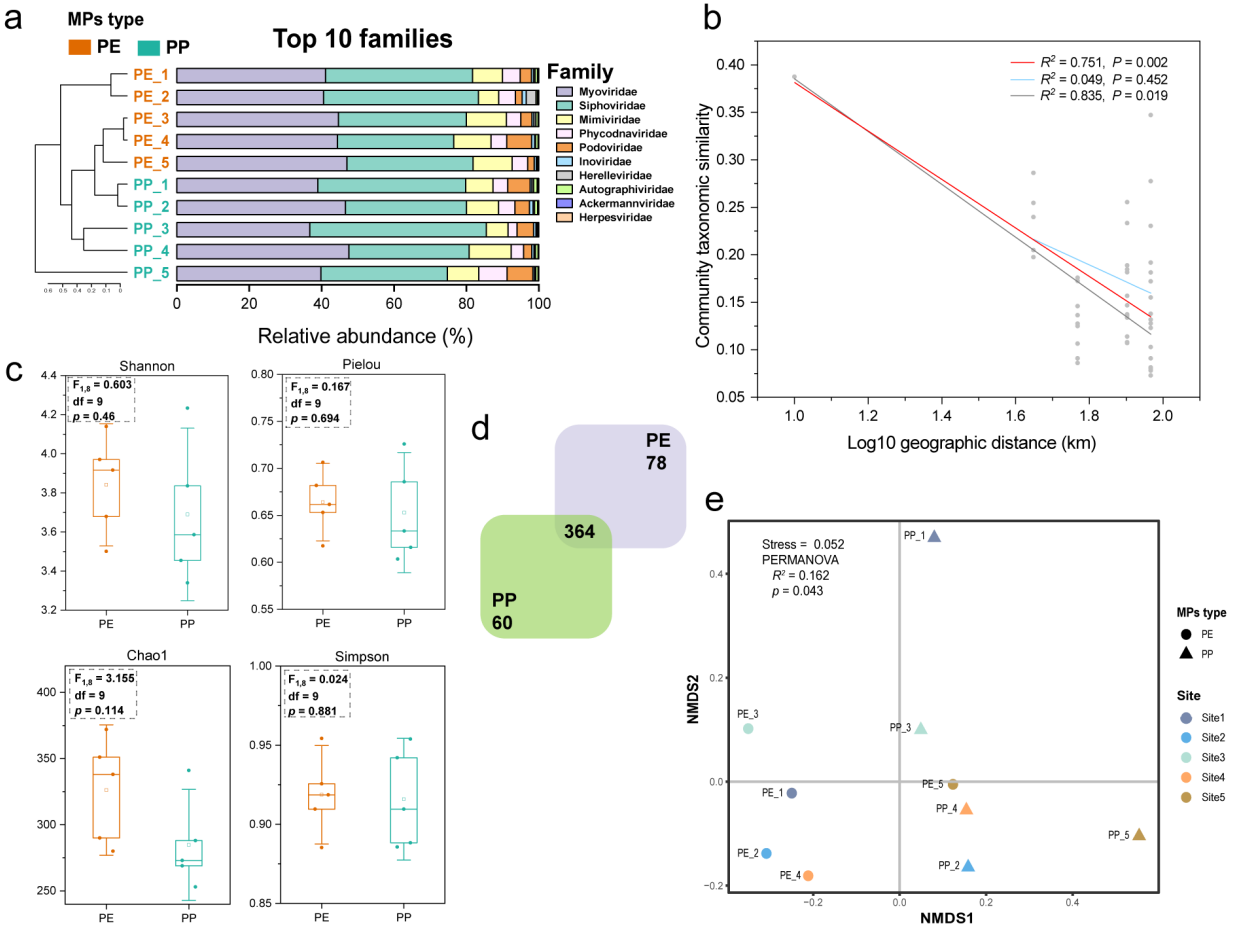
674 **Author Contributions Statement**

675 Ruilong Li designed the experiments and contributed to data analysis and the writing

of the paper. Xinli An performed viral DNA extraction, sequencing and identification and the writing of the paper. Yijin Wang contributed to the creation of the final figures and the writing of the paper. Zhugen Yang contributed to the writing of the paper and discussion of results. Jian-Qiang Su contributed to the writing of the paper. Jonathan Cooper contributed to the discussion of results. Yong-Guan Zhu conceived the idea of the study and contributed to the writing of the paper. All authors contributed to the review and editing of the paper.

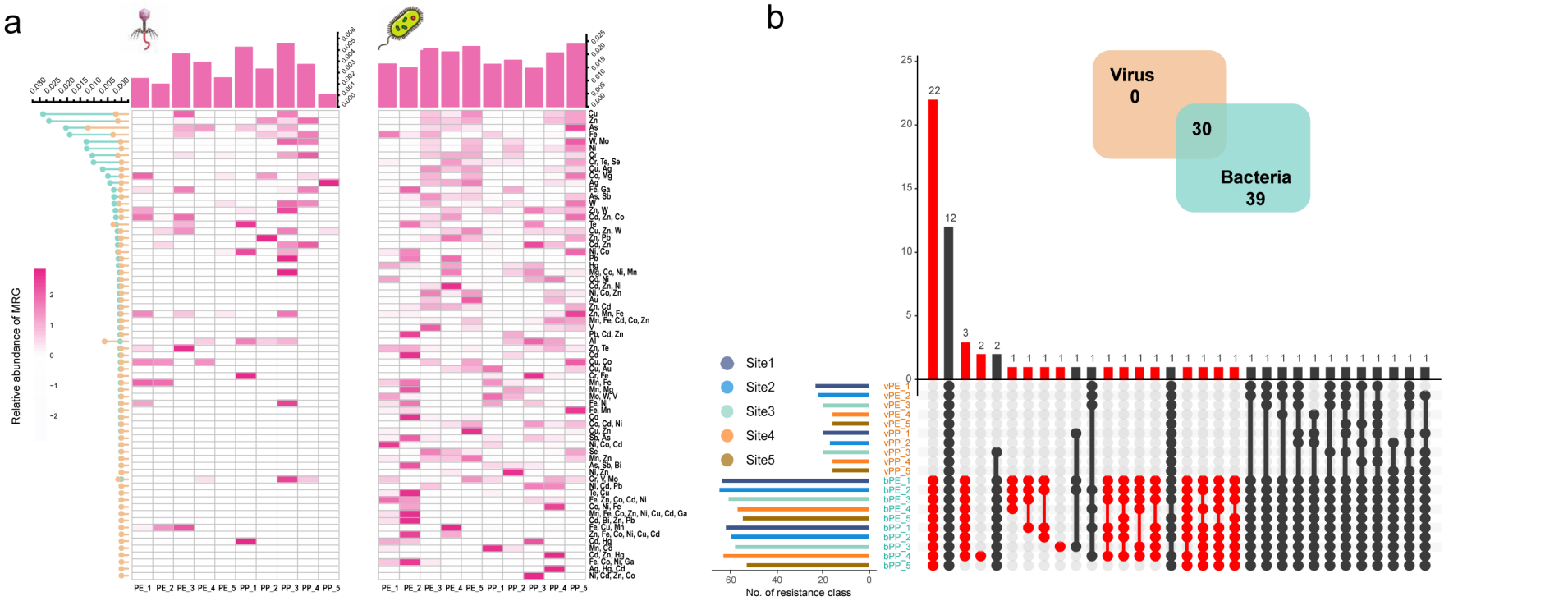
Competing Interests Statement

The authors declare no competing interests.


a
MPs type
PE
PP
Top 10 families
Family
Myoviridae
Siphoviridae
Mimiviridae
Phycodnaviridae
Podoviridae
Inoviridae
Herelleviridae
Autographiviridae
Ackermannviridae
Herpesviridae
PE_1
PE_2
PE_3
PE_4
PE_5
PP_1
PP_2
PP_3
PP_4
PP_5
0
20
40
60
80
100
Relative abundance (%)
b
R^2 = 0.751, P = 0.002
R^2 = 0.049, P = 0.452
R^2 = 0.835, P = 0.019
Community taxonomic similarity
Log10 geographic distance (km)
c
Shannon
$F_{1,8}$ = 0.603
df = 9
p = 0.46
Pielou
$F_{1,8}$ = 0.167
df = 9
p = 0.694
Chao1
$F_{1,8}$ = 3.155
df = 9
p = 0.114
Simpson
$F_{1,8}$ = 0.024
df = 9
p = 0.881
PE
PP
d
PE
78
364
PP
60
e
Stress = 0.052
PERMANOVA
R^2 = 0.162
p = 0.043
NMDS1
NMDS2
MPs type
PE
PP
Site
Site1
Site2
Site3
Site4
Site5

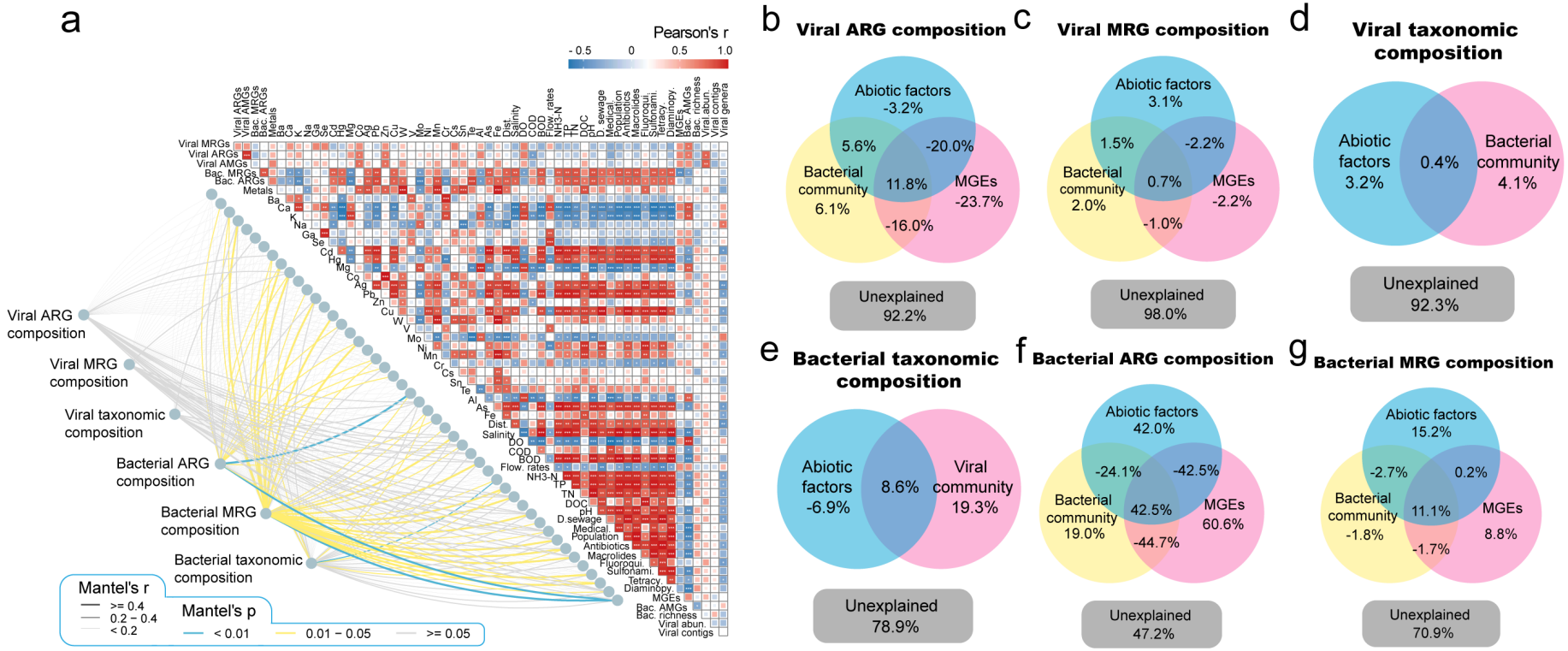
686

Fig. 1. Diversity and composition of viral communities. a Relative abundance of the top 10 abundant virus families in the two microplastic samples. The left Y-axis shows the UPGMA clustering based on Bray-Curtis distance. **b** Distance-decay relationships (DDRs) based on Bray-Curtis similarity (1 - dissimilarity) of viral taxonomic community compositions. **c** Differences in alpha diversity between PE and PP. (ANOVA, n=5, Shannon: $F_{1,8}$=0.603; df=9; p=0.460, Pielou: $F_{1,8}$=0.167; df=9; p=0.694, Chao1: $F_{1,8}$=3.155; df=9; p=0.114, Simpson: $F_{1,8}$=0.024; df=9; p=0.881). Data are presented as mean values ±SEM (Shannon for PE and PP: 3.84±0.11 and 3.69±0.16, Pielou for PE and PP: 0.66±0.01 and 0.65±0.02, Chao1 for PE and PP: 326.20±17.74 and 284.80±15.11, Simpson for PE and PP: 0.92±0.01 and 0.92±0.01). **d** Shared and unique virus genera between PE and PP. **e** Distribution patterns of virus communities visualized using NMDS analysis based on Bray-Curtis distance.


a
b
Relative abundance of MRG
PE_1 PE_2 PE_3 PE_4 PE_5 PP_1 PP_2 PP_3 PP_4 PP_5
Virus
0
30
Bacteria
39
Site1
Site2
Site3
Site4
Site5
No. of resistance class

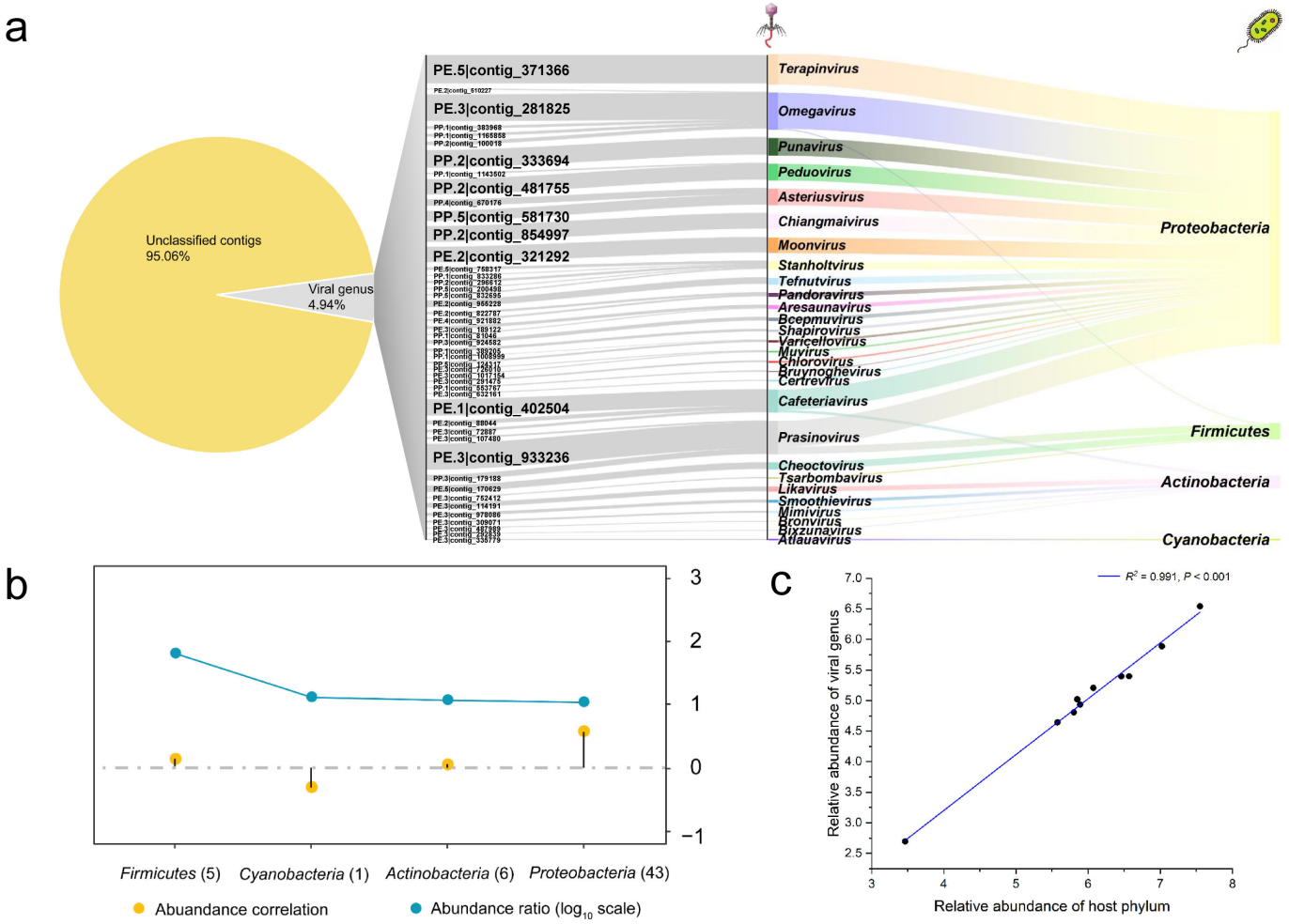
694

Fig. 2. Relative abundance (RPKM) of bacterial and viral-encoded resistance genes. a Heat map shows the relative abundance of the various metal resistance genes (MRGs) annotated. Bar chart above shows the relative abundance of MRGs in each sample. **b** Interference plots show MRGs in 20 classified groups (i.e. for bacterial and viral communities on PE, PP collected in 5 sampling sites). The bars in the bottom left corner show the number of resistance genes detected in the 20 groups. The upper bar indicates the intersection of resistance genes from different samples. The circles in the bottom graph matrix indicate the sets of groups with intersection. The Venn diagram in the top right corner shows the number of shared MRGs between the bacterial and viral communities.


a
Pearson's r
- 0.5
0
0.5
1.0
Viral ARG composition
Viral MRG composition
Viral taxonomic composition
Bacterial ARG composition
Bacterial MRG composition
Bacterial taxonomic composition
Mantel's r
>= 0.4
0.2 – 0.4
< 0.2
Mantel's p
< 0.01
0.01 – 0.05
>= 0.05
b
Viral ARG composition
Abiotic factors -3.2%
5.6%
-20.0%
Bacterial community 6.1%
11.8%
MGEs -23.7%
-16.0%
Unexplained 92.2%
c
Viral MRG composition
Abiotic factors 3.1%
1.5%
-2.2%
Bacterial community 2.0%
0.7%
MGEs -2.2%
-1.0%
Unexplained 98.0%
d
Viral taxonomic composition
Abiotic factors 3.2%
0.4%
Bacterial community 4.1%
Unexplained 92.3%
e
Bacterial taxonomic composition
Abiotic factors -6.9%
8.6%
Viral community 19.3%
Unexplained 78.9%
f
Bacterial ARG composition
Abiotic factors 42.0%
-24.1%
-42.5%
Bacterial community 19.0%
42.5%
MGEs 60.6%
-44.7%
Unexplained 47.2%
g
Bacterial MRG composition
Abiotic factors 15.2%
-2.7%
0.2%
Bacterial community -1.8%
11.1%
MGEs 8.8%
-1.7%
Unexplained 70.9%

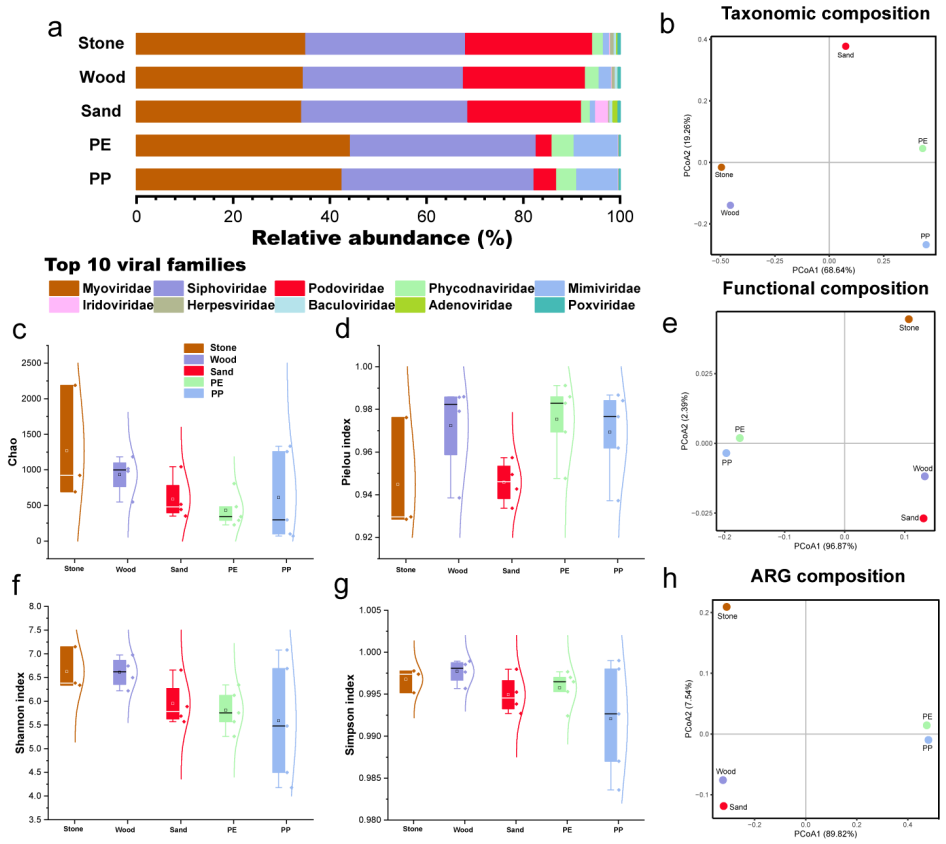
701

Fig. 3. MRG and taxonomic dynamics of bacterial and viral communities. a Pairwise comparisons of the biotic and abiotic variables. The color gradient in the heatmap denotes Pearson's correlation coefficients. Edge width corresponds to the Mantel's r statistic for the corresponding distance correlations, and edge color denotes the statistical significance. **b, c, d, e** Partial redundancy analysis differentiating the effects of abiotic factors, bacterial community and MGEs on ARG structures in bacterial and viral communities and the effects of abiotic factors, bacterial community and viral community on taxonomic structures in bacterial and viral communities.


a
Unclassified contigs
95.06%
Viral genus
4.94%
PE.5|contig_371366
PE.3|contig_281825
PP.2|contig_333694
PP.2|contig_481755
PP.5|contig_581730
PP.2|contig_854997
PE.2|contig_321292
PE.1|contig_402504
PE.3|contig_933236
Terapinvirus
Omegavirus
Punavirus
Peduovirus
Asteriusvirus
Chiangmaivirus
Moonvirus
Stanholtvirus
Tefnutvirus
Pandoravirus
Aresaunavirus
Bcepmuvirus
Shapirovirus
Varicellovirus
Muvirus
Chlorovirus
Bruynoghevirus
Certrevirus
Cafeteriavirus
Prasinovirus
Cheoctovirus
Tsarbombavirus
Likavirus
Smoothievirus
Mimivirus
Bronvirus
Bixzunavirus
Atlauavirus
Proteobacteria
Firmicutes
Actinobacteria
Cyanobacteria
b
3
2
1
0
−1
Firmicutes (5)
Cyanobacteria (1)
Actinobacteria (6)
Proteobacteria (43)
Abuandance correlation
Abundance ratio (log10 scale)
c
R2 = 0.991, P < 0.001
Relative abundance of viral genus
Relative abundance of host phylum
7.0
6.5
6.0
5.5
5.0
4.5
4.0
3.5
3.0
2.5
3
4
5
6
7
8

707

Fig. 4. Viral-host interaction structure. a Matched virus-host association. Association of specialized (one bacterial host and one virus), generic (one bacterial host and multiple viruses) and multivalent (multiple bacterial hosts and one virus) virus-host associations based on viral contig information. **b** Virus-host abundance (RPKM) correlations and abundance ratios. Solid circles indicate positive correlations while hollow circles indicate negative correlations. **c** The linear regression analysis between total relative abundance (RPKM) of viral genus and total relative abundance (RPKM) of predicted host phyla.


a
Stone
Wood
Sand
PE
PP
0
20
40
60
80
100
Relative abundance (%)
Top 10 viral families
Myoviridae
Siphoviridae
Podoviridae
Phycodnaviridae
Mimiviridae
Iridoviridae
Herpesviridae
Baculoviridae
Adenoviridae
Poxviridae
b
Taxonomic composition
PCoA1 (68.64%)
PCoA2 (19.26%)
c
Chao
d
Pielou index
e
Functional composition
PCoA1 (96.87%)
PCoA2 (2.39%)
f
Shannon index
g
Simpson index
h
ARG composition
PCoA1 (89.82%)
PCoA2 (7.54%)

713

714 **Fig. 5. Comparisons of viral community** composition (a), richness (c), and evenness (d, f, g) in natural particles and microplastics as well as the
715 dissimilarities of viral taxonomic and functional composition. (ANOVA, Shannon: $F_{1,19}$=4.515; df=20; p=0.047, Pielou: $F_{1,19}$=3.611; df=20;
716 p=0.073, Chao1: $F_{1,19}$=3.171; df=9; p=0.091, Simpson: $F_{1,19}$=2.327; df=20; p=0.144). Data are presented as mean values ±SEM (Shannon for
717 nature particles and MPs: 6.37±0.15 and 5.70±0.29, Pielou for nature particles and MPs: 0.96±0.01 and 0.97±0.01, Chao1 for nature particles and
718 MPs: 898.27±153.95 and 520.00±111.71, Simpson for nature particles and MPs: 1.00±0.00 and 0.99±0.00). Principal Coordinate Analysis (PCoA)
719 analysis based on bray-curtis distance for (b) viral taxonomic composition, (e) viral functional composition based on eggNOG database, and (h)
720 viral ARG composition based on SARG databas

References

1. Bank, M.S. & Hansson, S.V. The Plastic Cycle: A Novel and Holistic Paradigm for the Anthropocene. *Environmental science technology* **53**, 7177-7179 (2019).
2. Kim, S.W., Waldman, W.R., Kim, T. & Rilling, M.C. Effects of Different Microplastics on Nematodes in the Soil Environment: Tracking the Extractable Additives Using an Ecotoxicological Approach. *Environmental science & technology* **54** (2020).
3. Yuan, W. et al. Tracing and trapping micro- and nanoplastics: Untapped mitigation potential of aquatic plants? *Water research* **242**, 120249 (2023).
4. Roman, L., Christoph, W., Alke, P. & Barbara, R. Emergence of nanoplastic in the environment and possible impact on human health. *Environmental science technology* **53**, 1748-1765 (2019).
5. Frère, L. et al. Microplastic bacterial communities in the Bay of Brest: Influence of polymer type and size. *Environmental pollution* **242**, 614-625 (2018).
6. Zobell, C.E. & Anderson, D.Q. Observations on the multiplication of bacteria in different volumes of stored sea water and the influence of oxygen tension and solid surfaces. *The biological bulletin* **71**, 324-342 (1936).
7. Zettler, E.R., Mincer, T.J. & Amaral-Zettler, L.A. Life in the "plastisphere": microbial communities on plastic marine debris. *Environmental science & technology* **47**, 7137-7146 (2013).
8. Zhu, D., Ma, J., Li, G., Rillig, M.C. & Zhu, Y.-G. Soil plastispheres as hotspots of antibiotic resistance genes and potential pathogens. *The ISME journal* **16**, 521-532 (2022).
9. Bank, M.S., Ok Y.S. & Swarzenski, P.W. Microplastic's role in antibiotic resistance. *Science (New York, N.Y.)* **369**, 1315 (2020).
10. Lu, J., Yu, Z.G., Ngiam, L. & Guo, J.H. Microplastics as potential carriers of viruses could prolong virus survival and infectivity. *Water Research* **225**, 119115 (2022).
11. Ochirbat, E. et al. Heteroaggregation of virions and microplastics reduces the number of active bacteriophages in aqueous environments. *Journal of environmental quality* **52** (2023).
12. Moresco, V. et al. Binding, recovery, and infectiousness of enveloped and non-enveloped viruses associated with plastic pollution in surface water. *Environmental pollution (Barking, Essex : 1987)* **308**, 119594 (2022).
13. Li, R., Zhu, L., Cui, L. & Zhu, Y.-G. Viral diversity and potential environmental risk in microplastic at watershed scale: Evidence from metagenomic analysis of plastisphere. *Environment international* **161**, 107146 (2022).
14. Chen, Y. et al. Prokaryotic viruses impact functional microorganisms in nutrient removal and carbon cycle in wastewater treatment plants. *Nature Communications* **12**, 5398 (2021).
15. Pedro, B. et al. Dominance of phage particles carrying antibiotic resistance genes in the viromes of retail food sources. *The ISME journal* **17**, 195-203 (2022).
16. Debroas, D. & Siguret, C. Viruses as key reservoirs of antibiotic resistance genes in the environment. *The ISME journal* **13**, 2856-2867 (2019).
17. Christian, S. et al. Viromes outperform total metagenomes in revealing the spatiotemporal patterns of agricultural soil viral communities. *The ISME journal* **15**, 1956-1970 (2021).

18. Amaral-Zettler, L.A., Zettler, E.R. & Mincer, T.J. Ecology of the plastisphere. *Nature Reviews Microbiology* **18**, 139-151 (2020).
19. Ogonowski, M. et al. Evidence for selective bacterial community structuring on microplastics. *Environmental microbiology* **20**, 2796-2808 (2018).
20. Cheng, J. et al. Relative influence of plastic debris size and shape, chemical composition and phytoplankton-bacteria interactions in driving seawater plastisphere abundance, diversity and activity. *Frontiers in Microbiology* **11**, 610231 (2021).
21. Du, Y., Liu, X., Dong, X. & Yin, Z. A review on marine plastisphere: biodiversity, formation, and role in degradation. *Computational and Structural Biotechnology Journal* (2022).
22. Li, H.-Q. et al. Soil pH has a stronger effect than arsenic content on shaping plastisphere bacterial communities in soil. *Environmental Pollution* **287**, 117339 (2021).
23. Chevallereau, A., Pons, B.J., van Houte, S. & Westra, E.R. Interactions between bacterial and phage communities in natural environments. *Nature Reviews Microbiology* **20**, 49-62 (2022).
24. Liu, Z. et al. Viruses Regulate Microbial Community Assembly Together with Environmental Factors in Acid Mine Drainage. *Applied and Environmental Microbiology* **89**, e01973-01922 (2023).
25. Gao, S. et al. Patterns and ecological drivers of viral communities in acid mine drainage sediments across Southern China. *Nature Communications* **13**, 2389 (2022).
26. Chen, M.-L. et al. Viral community and virus-associated antibiotic resistance genes in soils amended with organic fertilizers. *Environmental Science & Technology* **55**, 13881-13890 (2021).
27. Wommack, K.E. et al. VIROME: a standard operating procedure for analysis of viral metagenome sequences. *Standards in genomic sciences* **6**, 421-433 (2012).
28. Finke, J.F., Hunt, B.P., Winter, C., Carmack, E.C. & Suttle, C.A. Nutrients and other environmental factors influence virus abundances across oxic and hypoxic marine environments. *Viruses* **9**, 152 (2017).
29. Liang, X., Wang, Y., Zhang, Y., Zhuang, J. & Radosevich, M. Viral abundance, community structure and correlation with bacterial community in soils of different cover plants. *Applied Soil Ecology* **168**, 104138 (2021).
30. Han, L. et al. Genetic and functional diversity of ubiquitous DNA viruses in selected Chinese agricultural soils. *Scientific reports* **7**, 45142 (2017).
31. Télesphore, S. Environmental bacteriophages: viruses of microbes in aquatic ecosystems. *Frontiers in microbiology* **5**, 355 (2014).
32. Lu, J. et al. Metagenomic analysis of viral community in the Yangtze River expands known eukaryotic and prokaryotic virus diversity in freshwater. *Virologica Sinica* **37,** 60-69 (2022).
33. Marine, R. et al. Caught in the middle with multiple displacement amplification: the myth of pooling for avoiding multiple displacement amplification bias in a metagenome. *Microbiome* **2**, 3 (2014).
34. Yang, Y., Li, T., Liu, P., Li, H. & Hu, F. The formation of specific bacterial communities contributes to the enrichment of antibiotic resistance genes in the soil plastisphere. *Journal of Hazardous Materials* **436**, 129247 (2022).
35. Chen, M.-L. et al. Viral community and virus-associated antibiotic resistance genes

in soils amended with organic fertilizers. *Environmental Science & Technology* **55**, 13881-13890 (2021).

36. Wu, Z. Distinct adaptive strategies and microbial interactions of soil viruses under different metal(loid) contaminations. *Journal of Hazardous Materials* **460**, 132347 (2023).

37. Qi, R. et al. Heavy metal(loid)s shape the soil bacterial community and functional genes of desert grassland in a gold mining area in the semi-arid region. *Environmental research* **214**, 113749 (2022).

38. Yao, Y. et al. Cross-regional scale pollution of freshwater biofilms unveiled by antibiotic resistance genes. *Science of The Total Environment* **818**, 151835 (2022).

39. Krupovic, M., Prangishvili, D., Hendrix, R.W. & Bamford, D.H. Genomics of bacterial and archaeal viruses: dynamics within the prokaryotic virosphere. *Microbiology and molecular biology reviews* **75**, 610-635 (2011).

40. Liao, H. et al. Response of soil viral communities to land use changes. *Nature Communications* **13**, 6027 (2022).

41. Li, Z. et al. Deep sea sediments associated with cold seeps are a subsurface reservoir of viral diversity. *The ISME journal* **15**, 2366-2378 (2021).

42. Rillig, M. C., Kim, S. W. & Zhu, Y.-G. The soil plastisphere. *Nature reviews. Microbiology* (2023).

43. Adams, R. I., Bateman, A. C., Bik, H. M. & Meadow, J. F. Microbiota of the indoor environment: a meta-analysis. *Microbiome* **3**, 49 (2015).

44. Ter Horst, A. M., Fudyma, J. D., Sones, J. L. & Emerson, J. B. Dispersal, habitat filtering, and eco-evolutionary dynamics as drivers of local and global wetland viral biogeography. *The ISME journal* **17**, 2079-2089 (2023).

45. Yuan, Q. et al. UV-aging of microplastics increases proximal ARG donor-recipient adsorption and leaching of chemicals that synergistically enhance antibiotic resistance propagation. *Journal of hazardous materials* **427**, 127895 (2022).

46. Xu, C., Lu, J., Shen, C., Wang, J. & Li, F. Deciphering the mechanisms shaping the plastisphere antibiotic resistome on riverine microplastics. *Water Research* **225**, 119192 (2022).

47. Castaño-Ortiz, J. M. et al. Fate of pharmaceuticals in the Ebro River Delta region: The combined evaluation of water, sediment, plastic litter, and biomonitoring. *Science of the Total Environment* **906**, 167467 (2024).

48. Andersson, D. I.et al. The biological cost of antibiotic resistance. *Current Opinion in Microbiology* **2**, 489-493 (1999).

49. Yang, K. et al. Temporal dynamics of antibiotic resistome in the plastisphere during microbial colonization. *Environmental science & technology* **54**, 11322 (2020).

50. Li, R. et al. Impact of urbanization on antibiotic resistome in different microplastics: evidence from a large-scale whole river analysis. *Environmental Science & Technology* **55**, 8760-8770 (2021).

51. Martin, M. Cutadapt removes adapter sequences from high-throughput sequencing reads. *EMBnet. journal* **17**, 10-12 (2011).

52. Li, D. et al. MEGAHIT v1. 0: a fast and scalable metagenome assembler driven by advanced methodologies and community practices. *Methods* **102**, 3-11 (2016).

53. Noguchi, H., Taniguchi, T. & Itoh, T. MetaGeneAnnotator: detecting species-specific patterns of ribosomal binding site for precise gene prediction in anonymous prokaryotic

and phage genomes. *DNA research* **15**, 387-396 (2008).

54. Li, W. & Godzik, A. Cd-hit: a fast program for clustering and comparing large sets of protein or nucleotide sequences. *Bioinformatics* **22**, 1658-1659 (2006).

55. Li, H. & Durbin, R. Fast and accurate short read alignment with Burrows–Wheeler transform. *Bioinformatics* **25**, 1754-1760 (2009).

56. Huson, D.H., Mitra, S., Ruscheweyh, H.-J., Weber, N. & Schuster, S.C. Integrative analysis of environmental sequences using MEGAN4. *Genome research* **21**, 1552-1560 (2011).

57. Trubl, G. et al. Towards optimized viral metagenomes for double-stranded and single-stranded DNA viruses from challenging soils. *PeerJ* **7**, e7265 (2019).

58. Adriaenssens, E.M. et al. Environmental drivers of viral community composition in Antarctic soils identified by viromics. *Microbiome* **5**, 1-14 (2017).

59. Bolger, A. M. et al. Trimmomatic: a flexible trimmer for Illumina sequence data. *Bioinformatics* **30**, 2114-2120 (2014).

60. Uritskiy, G.V., DiRuggiero, J. & Taylor, J. MetaWRAP—a flexible pipeline for genome-resolved metagenomic data analysis. *Microbiome* **6**, 1-13 (2018).

61. Patro, R., Duggal, G., Love, M.I., Irizarry, R.A. & Kingsford, C. Salmon provides fast and bias-aware quantification of transcript expression. *Nature methods* **14**, 417-419 (2017).

62. Edwards, R.A., McNair, K., Faust, K., Raes, J. & Dutilh, B.E. Computational approaches to predict bacteriophage–host relationships. *FEMS microbiology reviews* **40**, 258-272 (2016).

63. Pons, J. C. et al. VPF-Class: taxonomic assignment and host prediction of uncultivated viruses based on viral protein families. *Bioinformatics* **37**, 1805-1813 (2021).

64. Laslett, D. & Canback, B. ARAGORN, a program to detect tRNA genes and tmRNA genes in nucleotide sequences. *Nucleic acids research* **32**, 11-16 (2004).

65. Camacho, C. et al. BLAST+: architecture and applications. *BMC Bioinformatics* **10**, 1-9 (2009).

66. Seemann, T. et al. Prokka: rapid prokaryotic genome annotation. *Bioinformatics* **30**, 2068-2069 (2014).



https://dspace.org/

Viral metagenome reveals microbial hosts and the associated antibiotic resistome on microplastics

Li, Ruilong; An, Xin-Li; Wang, Yijin; Yang, Zhugen; Su, Jian-Qiang ...

2024-06-01
Springer
https://doi.org/10.1038/s44221-024-00249-y
Li R, An XL, Wang Y, et al., (2024) Viral metagenome reveals microbial hosts and the associated antibiotic resistome on microplastics. Nature Water, Volume 2, June 2024, pp. 533-565

Downloaded from a DSpace repository. https://dspace.org/